

# Computational Adaptation Model and its Predictions for Color Induction of First and Second Orders

*Hedva Spitzer and Yuval Barkan*

*Dept. of Biomedical Engineering, Faculty of Engineering, Tel-Aviv University  
Tel-Aviv, Israel*

## Abstract

The appearance of a patch of color or its contrast depends not only on the stimulus itself but also on the surrounding stimuli (induction effects). We suggest that these induction effects are epi-phenomena of color constancy (first order color adaptation) and color contrast discrimination (second order color adaptation) mechanisms. Despite accumulated electrophysiological and psychophysical findings on the role of the surrounding color and contrast on the perceived central stimulus, no previous models have been proposed which integrate this data. A comprehensive computational physiological model is presented which describes the retinal and cortical color-coded receptive fields and their local and remote adaptation mechanisms. The model's predictions for both induction effects, color induction and contrast induction, are presented. The model also predicts the effect of variegated surrounding on the central perceived color.

## 1. Introduction

The appearance of a visual stimulus depends not only on the stimulus itself but also on other surrounding and remote stimuli. Induction (simultaneous contrast) and contrast induction are among the important appearance phenomena related to the spatial surrounding effects. Induction is the psychophysical phenomenon of the change in the appearance of a color (or an achromatic stimulus) caused by the presence of a surrounding stimulus. Color contrast induction is the modulating effect of the surrounding contrast on the perceived contrast of the central area.<sup>1,2</sup> Color contrast is the distance between colors on a perceptual uniform color space, such as that of Derrington et al.<sup>3</sup> The "intermixed" effect, i.e. the different perceived color effect due to a variegated (textured chromatic field) surround vs. a homogeneous surround while the surround is composed of the same average chromaticity and intensity at both surround areas has also been studied.<sup>4,6</sup> These color and color contrast effects have been tested by many groups and are well known (mainly color induction). However, their physiological mechanism and computational aspects are in dispute or yet unknown. Color induction is widely accepted to be associated with the very well known phenomenon of color constancy system can partly discount illumination. In this study we

attempt to claim and demonstrate that color induction is an epi-phenomenon of color constancy, since the same mechanism causes both effects. Contrast induction is suggested as a mechanism for enhancing the differences in contrast surfaces or objects. Thus, both mechanisms serve for enhancing the differences between the stimulus and its surrounding area.

We suggest a comprehensive computational model based on the retinal and cortical color-coded receptive fields (RF) and on first order (retinal)<sup>7,8</sup> and second order (cortical) adaptation mechanisms.<sup>9</sup> The model is based on the physiological color-coded cells, the opponent (retinal) and the double-opponent (cortical cells). The first part of the model, the first order, which is based on the color-opponent cells, is described here briefly, since it has been described previously as a color constancy model.<sup>7,8</sup> The second part of the model is based on the 'double-opponent' (do) receptive fields of the visual cortex, which have been encountered in the V1 and V2 areas, whose inputs are the responses of the opponent cells. Thus, a double-opponent cell is fed by an On cell type receptive field to its center region and an Off cell with the same chromaticity properties to its surround region.<sup>9</sup>

### 1.1 Color Induction

The influence of the color of peripheral areas on the perceived color of a central area is regarded here as the first order of color adaptation.<sup>8,10</sup> This effect has also been found electrophysiologically on the single cell level in the lateral geniculation nucleus (LGN).<sup>11,12</sup>

Several studies have demonstrated that the shift in color appearance due to color induction is in a direction complementary to the inducing stimulus.<sup>10,13,14</sup> This trend was found for the three cardinal directions as well as for the non-cardinal directions,<sup>13</sup> although previous studies have shown some deviations from this rule using different paradigms.<sup>15</sup> A debate concerning the neuronal locus of color induction has been ongoing for some time.<sup>16</sup> In this study we demonstrate that this logic, concerning the locus of color induction, is not necessarily valid, due to the predictions of a model based on color-coded opponent cells.<sup>7,8</sup>

### 1.2 Contrast-Contrast Induction

Psychophysical and electrophysiological findings show the existence of the second order adaptation, i.e.

contrast- contrast adaptation, with basic adaptation properties somewhat similar to first order effects, such as the role of the remote area.<sup>1,16-19</sup> The color contrast induction results implied the existence of an interocular transfer of color contrast induction, suggesting a cortical locus. More direct evidence on the locus of the effect was derived from findings on the role of the remote area and its chromatic properties outside the “classical receptive field” single cells in the V4 area.<sup>17</sup> The two suggested color adaptation mechanisms are modeled as gain control mechanisms based on the “curve-shifting” effect.<sup>7, 8, 20-22</sup>

## 2. The Model

The model is presented in three main stages, Fig. 1. The first stage (2.1) describes the transformation of visual stimuli into retinal ganglion cells responses of three types of color-coded On-center cells. The second stage (2.2) describes the cortical double-opponent color-coded cells, which are fed by the responses of the first stage, and the remote adaptation mechanism which acts on their responses. The third stage (2.3) calculates a transformation of these cells’ activity levels to a perceived image, in a standard CIE notation (XYZ) or RGB scale. This is performed through an inverse function.

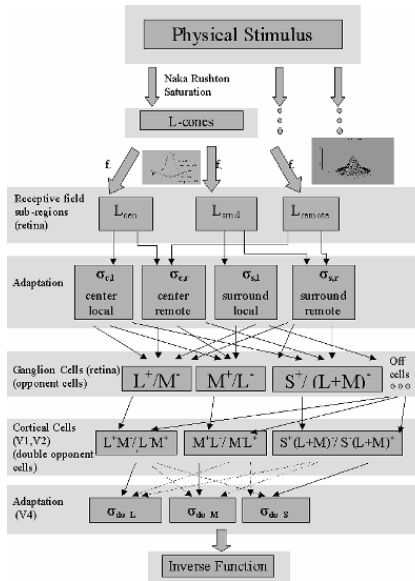


Figure 1. Schematic diagram of the suggested model.

### 2.1. Responses of Three Types of On-Center Color-Coded Cells, The First Order

The retinal ganglion cells’ responses form the last chain of data processing in the retina. They receive their input from the cones through several processing layers. These cells have a color-opponent receptive field with a center-surround spatial structure. (A receptive field (RF) is that region in the visual field from which a visual stimulus will elicit a response.) The cells considered here belong to the three most common color-coded types in the retina. These cell types are labeled  $L^+M^-$ ,  $M^+L^-$  and  $S^+(L+M)^-$ , with L, M and S standing for long, medium and short wavelength sensitivity, respectively. For example, an  $S^+(L+M)^-$  cell has an excitatory S (‘blue’) response in its

center and an inhibitory (L+M) (‘yellow’) response in its surround.<sup>23</sup>

The spatial response profile of the two sub-regions of the RGCs’ RF, ‘center’ and ‘surround’, is expressed by the commonly used Difference-of-Gaussians (DOG), performed only after each sub-region is adapted, as follows: The ‘Center’ signals for the three spectral regions,  $L_{cen}$ ,  $M_{cen}$  and  $S_{cen}$ , that feed the RGC level are defined as an integral of the cones’ quantum catches, over the center sub-region, with a Gaussian decaying spatial weight function,  $f_c(x-x_0, y-y_0)$ <sup>21</sup>:

$$\begin{aligned} L_{cen}(x_0, y_0) &= \iint_{cen-area} L_{cone}(x, y) f_c(x-x_0, y-y_0) dx dy \\ M_{cen}(x_0, y_0) &= \iint_{cen-area} M_{cone}(x, y) f_c(x-x_0, y-y_0) dx dy \\ S_{cen}(x_0, y_0) &= \iint_{cen-area} S_{cone}(x, y) f_c(x-x_0, y-y_0) dx dy \end{aligned} \quad (1)$$

$f_c$  is defined as a Gaussian function. The ‘Surround’ signals  $L_{srnd}$ ,  $M_{srnd}$  and  $(L+M)_{srnd}$  are similarly defined, with a spatial weight function three times larger in diameter than that of the ‘center’.

The ‘Remote’ signal ( $L_{remote}$ ,  $M_{remote}$ ,  $S_{remote}$  and  $(L+M)_{remote}$ ) represents the peripheral area that extends far beyond the borders of the RF of the RGC and is defined as an integral of the cones’ quantum catches over the remote area, with a different Gaussian decaying spatial weight function.<sup>7,8,12,22</sup> The four ‘remote’ signals are:

$$\begin{aligned} L(remote) &= \iint_{remote area} L_{cone}(x, y) f_r(x, y) dx dy \\ M(remote) &= \iint_{remote area} M_{cone}(x, y) f_r(x, y) dx dy \\ S(remote) &= \iint_{remote area} S_{cone}(x, y) f_r(x, y) dx dy \\ (L+M)(remote) &= \iint_{remote area} (L+M)_{cone}(x, y) f_r(x, y) dx dy \end{aligned} \quad (2)$$

The ‘remote’ area has the shape of an annulus, concentric to that of the ‘center’ and the ‘surround’. The color-coded ‘center’ and ‘surround’ sub-regions adapt separately, before the subtraction operation between their responses, as shown physiologically.<sup>21,22</sup> The response,  $R$ , of each of the On-center color coded cells was therefore expressed by:

$$R_{op}(G, t) = \frac{G_{cen}(t)}{G_{cen}(t) + \sigma_{cen}(G_{cen}(t))} - \frac{G_{srnd}(t)}{G_{srnd}(t) + \sigma_{srnd}(G_{srnd}(t))} \quad (3)$$

where  $G$  is the signal (of each of the color-coded cells, L, M and S) feeding the ‘center’ or the ‘surround’ sub-regions and  $\sigma$  is used here as the adaptation factor instead of the ‘saturation constant’ of the Naka-Rushton equation.<sup>7,22</sup> The dependence of  $\sigma$  as function of the history of the stimulation was taken here as a “curve-shifting” mechanism composed of local,  $\sigma_l$  and remote  $\sigma_r$  components (for example, at steady state, for channel L,  $\sigma_{L,cen}(t=\infty) = \sigma_{L,local} + \sigma_{L,remote}$  where  $\sigma_{L,local} = \alpha L_{cen} + \beta$  and  $\sigma_{L,remote} = C_{cen} L_{remote}$  and  $\alpha$ ,  $\beta$  and  $C$  are constants). The linear dependence of  $\sigma$  was chosen in order to obtain Weber law for specific cases, as described previously.<sup>7,8,22</sup> Such a mechanism would contribute to a reduction in the chromatic illumination and would cause color induction.

A color-opponent cell's response  $R_{op}$  ( $R_{op} = R(G,t)$ ), is the subtraction between the responses of the center and the surround of each retinal ganglion cell type after adaptation for each subregion separately. For On-center cells the response is expressed as  $L^+/M^-$ ,  $M^+/L^-$  and  $S^+(L+M)^-$ , and for Off-center cells as  $L^-M^+$ ,  $M^-L^+$  and  $S^-(L+M)^+$ .

## 2.2 Double-Opponent Cells, The Second Order:

The double-opponent cell is composed of a center receptive field, for example  $L_{do-c}$  ("do-center" (do-c) signal) from the first group of On-center ganglion cells located in a do-center area, and receives its own surround response  $L_{do-s}$  ("do-surround" (do-s) signal) from a corresponding group of Off-center cells (e.g.,  $L^-M^+$ ) located in a do-surround area.

$$\begin{aligned} L_{(do-c)} &= \iint_{center\_do\_area} R_{op(l+)}(x,y) f_{(do-c)}(x,y) dx dy \\ M_{(do-c)} &= \iint_{center\_do\_area} R_{op(m+)}(x,y) f_{(do-c)}(x,y) dx dy \\ S_{(do-c)} &= \iint_{center\_do\_area} R_{op(s+)}(x,y) f_{(do-c)}(x,y) dx dy \end{aligned} \quad (4)$$

where the responses of  $R_{op(l+)}(x,y)$ ,  $R_{op(m+)}(x,y)$ ,  $R_{op(s+)}(x,y)$  are actually the opponent cell responses and were determined by spatial as well as spectral properties at each  $x,y$  location convoluted with  $f_{(do-c)}$ , the weight function of the center sub-region of each double-opponent cell.  $f_{(do-c)}$  has a Gaussian spatial-weight function. A similar mathematical formulation for the three-color do-surround expressions is calculated, by the Off-cell responses.

The double-opponent responses (or "do-outputs") of the three On-center, double-opponent color-coded cells:  $L^+M^-/L^-M^+$ ,  $M^+L^-/M^-L^+$ ,  $S^+(L+M)^-/S^-(L+M)^+$ , before the adaptation stage, are given by:

$$\begin{aligned} L_{do} &= L_{(do-c)} - M_{(do-s)} \\ M_{do} &= M_{(do-c)} - L_{(do-s)} \\ S_{do} &= S_{(do-c)} - (L_{(do-s)} + M_{(do-s)}) \end{aligned} \quad (5)$$

### Remote Area:

The 'remote' signal represents the peripheral area which extends far beyond the borders of the double-opponent classical receptive field of the V4 area 18. The 'remote' area has the shape of an annulus around the entire RF region. The four remote signals ( $L_{(do-remote)}$ ,  $M_{(do-remote)}$ ,  $S_{(do-remote)}$  and  $(L+M)_{(do-remote)}$ ) are defined in Eq. 6 as the convolution or inner product of each absolute response at each location of the remote area of the double-opponent cell signal. The four 'remote' signals,  $L_{remote}$ ,  $M_{remote}$ ,  $S_{remote}$  and  $(L+M)_{remote}$  that feed the double-opponent cells level, were defined as:

$$\begin{aligned} L_{(do-remote)} &= \iint_{remotearea} |L_{(do)}(x,y)| f_r(x,y) dx dy \\ M_{(do-remote)} &= \iint_{remotearea} |M_{(do)}(x,y)| f_r(x,y) dx dy \\ S_{(do-remote)} &= \iint_{remotearea} |S_{(do)}(x,y)| f_r(x,y) dx dy \\ (L+M)_{(do-remote)} &= \iint_{remotearea} |Y_{(do)}(x,y)| f_r(x,y) dx dy \end{aligned} \quad (6)$$

where  $L_{(do)}(x,y)$ ,  $M_{(do)}(x,y)$ ,  $S_{(do)}(x,y)$  and  $Y_{(do)}(x,y) = (L+M)_{(do)}(x,y)$  are spatial and spectral responses at each  $x, y$  which act on the do-remote areas.<sup>17</sup>

### Adaptation:

The color-coded double-opponent cells are adapted (Eqs. 7,8) by a suggested remote adaptation mechanism in a manner similar to a mechanism based on psychophysical findings, as shown in Singer and D'Zmura<sup>1,2</sup> who found that modulating the contrast of an annulus induces an apparent modulation of the color contrast of a central disk. The mechanism for adaptation by a "curve-shifting" mechanism at the level of cortical color-coded cells, (contrast adaptation, i.e. second order), is similar to the adaptation at the retinal level.

$$R_{(do-a)}(G,t) = R_{max} \frac{G_{do}(t)}{|G_{do}(t)| + \sigma G_{do-remote-b,t}} \quad (7)$$

where,

$$\sigma = c G_{do-remote-b} + \beta \quad (8)$$

and where  $G_{do-remote-b}$  stands for the temporal dependence of  $L_{do-remote}$ ,  $M_{do-remote}$  and  $S_{do-remote}$  of the remote regions of the double-opponent receptive fields and determines the dynamic adaptation.  $G_b$  is the temporal dependence. The constant  $C$  describes the degree of 'curve-shifting', i.e., it determines the shift of the response curve after a certain amount of contrast has been viewed.

## 2.3 Transformation of the Adapted Color-Coded Cells' Response to a Perceived Image

This procedure is used for inversely calculating the functions of the adapted double-opponent and opponent responses to the cone responses and RGB scale in order to observe the outcome of the model on real images.<sup>9</sup> The calculated perceived color contrast is the color contrast that would stimulate the triplet of  $L'_{do}$ ,  $M'_{do}$ ,  $S'_{do}$  to the same perceived contrast responses, while the contrast in the "remote" areas ( $L'_{do-remote}$ ,  $M'_{do-remote}$  and  $S'_{do-remote}$ ) is equal to that in the corresponding double-opponent areas.

$$L'_{do-remote} = |L'_{do}| \quad M'_{do-remote} = |M'_{do}| \quad S'_{do-remote} = |S'_{do}| \quad (9)$$

Thus, the inverse function from the opponent cells' responses to cone values was performed assuming that a uniform achromatic surface was presented in their 'remote' area.<sup>7,8</sup> The adapted cone responses may then be converted to the CIE RGB color space or to any other color space.<sup>23</sup>

## 3. Simulations and Results

### 3.2 Performance of the Model: Psychophysical Predictions

#### 3.2.1 Predictions of First-Order Color Adaptation

Figure 2 demonstrates the calculated perceived color (colored circles) at the central gray stimulus (the demonstrations at the left and bottom to the curve figure), while different surrounding colors (colored stars) were given. The predictions on the induction effect were performed with two degrees of the model's performance by applying two different values of  $\beta$ , which reflect two strengths of the adaptation parameter  $\sigma$  of the first order adaptation mechanism.

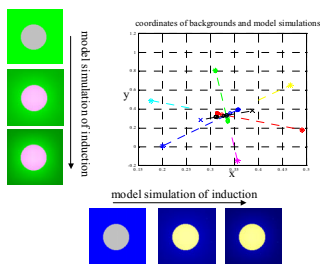


Figure 2. The model's predictions for different chromatic surrounding stimuli (the colored stars).

### 3.2.2 Predictions of Second-Order Color Adaptation

Figure 3 presents simulations of two examples of the model's ability to predict the perceived color contrast automatic modulation due to the surrounding contrast model's, and thus its ability to dual effect on the central contrast towards suppression (upper line) or enhancement (bottom line), as found psychophysically.<sup>24,25</sup> The model can also predict the color modulation for textures which are not constructed from cardinal colors, as found psychophysically.<sup>2</sup>

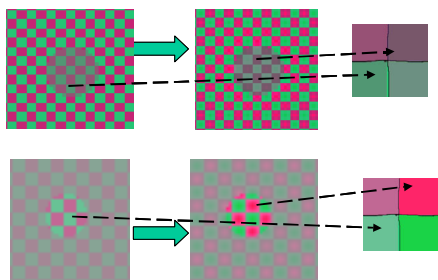


Figure 3. Demonstration of the model's prediction (second column) for central contrast suppression (lower row) and enhancement (upper row) due to the surrounding inducing contrast (left column).

### 3.2.3 Effect of Textured Chromatic Surround on the Perceived Color

We consider also the variegated induction as consisting of two types of inductions, the induction of the average color of the surrounding region and the induction of the surrounding contrast on the perceived central contrast. Since the first induction (due to the average color of the surrounding) causes induction towards the complementary color and is processed first, the second induction (contrast-contrast), which receives its input from the output of the first mechanism, acts on a different contrast channel regarding the central area.

Due to the above and observed interaction effect<sup>5,6,26</sup> an additional component ( $d < 1$ ) was added to the contrast adaptation mechanism. Accordingly, Eq. 8 is replaced by Eq. 10, and is demonstrated for the color contrast channel L/M:

$$\sigma_{do-remoteb}(t) = \sigma_{L-remote} + d \cdot \sigma_{S/(L+M)-remote} \quad (10)$$

The same considerations and calculations were applied for the other color contrast channel, i.e. S/(L+M).

Figure 4c,d demonstrates the model's prediction (lower row) of having a smaller induction effect while the surrounding region is composed of variegated components compared to the effect from a homogenous surrounding region.

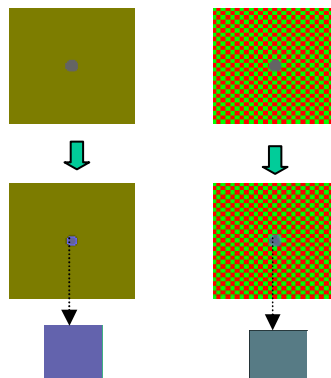


Figure 4. The model's prediction to yield a smaller induction effect while the surround area is variegated (right column).

## 4. Discussion and Conclusions

A computational biological model based on physiological retinal and cortical color-coded receptive fields and physiological adaptation mechanisms of the first and second order is presented. This order of color processing, of first dealing with the color and then with the color contrast, has a computational advantage, since color correction and enhancement become more cost-effective. This first order adaptation enables the visual system to first perform perceived color calculations and color constancy, which actually reduce the colored illumination. Only then is the second order adaptation, the modulation of contrast in order to enhance the change in color texture and color differences, performed. We have demonstrated that modulation of color contrast can affect the perceived color to some extent. This is also true for the calculated intensity contrast and the perceived intensity.

The issue of a different effect of the variegated vs. the homogenous surround on the perceived color also became relevant in judging or evaluating different color constancy models, many of which only took the average color of the surrounding areas into account, such as the different Retinex models and recent physiological color constancy models.<sup>7,8</sup> In conclusion, the predictions of induction effects and outcome algorithms applied to real images (Fig. 5) support the suggested comprehensive physiological model.



Figure 5. A demonstration that the physiological model can also be an effective algorithm for color constancy and for enhancement of color contrast on real images.

## Acknowledgements

This research was partly supported by the United States-Israel Bi-National Science Foundation (BSF).

## References

1. Singer, B. & D'Zmura, M. (1994) *Vision Res.* **34**, 3111-3126.
2. D'Zmura M., & Singer B. J (1996) *Opt Soc Am A* **13**, 2135-2140.
3. Derrington, A.M., Krauskopf, J. & Lennie, P. (1984) *J. Physiol.* **357**, 241-265.
4. Zaidi, Q., Spehar, B. & DeBonet J. (1998) *J Opt Soc Am A Opt Image Sci Vis.* **15**, 23-32.
5. Shevell, S. & wei, J. (1998) *Vision Res.* **38**, 1561-1566.
6. Brenner, E. & Cornelissen, F. W. (2002) *Perception*, **31**, 225-232.
7. Spitzer, H., & Rosenbluth, A. (2002) *Spatial Vision*, **15**, 277-302.
8. Spitzer, H. & Semo, S. (2002) *Pattern Recognition*, **35**, 1645-1659.
9. Spitzer, H. & Sherman, E. (2002) CGIV 2002, The first european conference on colour in graphics, image and vision.
10. Semo, S., Rosenbluth, A. & Spitzer H. (1998) *Perception* **27**, suppl. 43.
11. Creutzfeldt, O. D., Kastner J. M. C., Chao-Yi Li, S. & Pei, X. (1991) *Exp. Brain Res.* **87**, 3-21.
12. Creutzfeldt, O. D., Kastner, S., Pei, X. & Valberg A. (1991) *Exp. Brain Res.*, **87**, 22-45.
13. Krauskopf, J., Zaidi, Q. & Mandler, M. (1986) *Josa A*, **3**, 1752-1757.
14. Webster, M. A. & Mollon, J. D. (1995) *Nature* **373**, 694-698.
15. Ware, C. & Cowan, W. (1982). *Vision Res.* **22**, 1353-1362.
16. Zaidi, Q. C. (1999) In *Color Vision from genes to perception*. Cambridge university press.
17. Schein, S. J. & Desimone, R. (1990) *J. of Neuroscience* **10**, 3369-3389.
18. Chubb, C., Sperling, G. & Solomon, J. (1989) *Proc. Nat. Sc. USA*, **86**, 9631-9635.
19. Bonet, J. S. & Zaidi, Q. (1997) *Vision Res.* **37**, 1141-55.
20. Sakmann, B. and Creutzfeldt, O. D. (1969) *Plügers Arch.* **313**, 168-185.
21. Shapley, M. & Enroth-Cugell, C. (1984) *Progress in retinal Res.* **3**, 263-346.
22. Dahari, R., & Spitzer, H. (1996) *JOSA A* **13**, 419-439.
23. Wyszecki, G. & Stiles, W. S. (1982). In *Color Science: Concepts and Methods, Quantitative Data and Formulae*. John Wiley & Sons.
24. Xing, J. & Heeger, D. J. (2001) *Vision Res.* **41** 5 571-583.
25. D'Zmura, M. & Singer, B. (1999) in: *Color Vision from genes to perception*. Edited by: K.R. Gegenfurtner and L.T.Sharpe. Cambridge university press.
26. Brown, R. O. & MacLeod, D. I. A. (1997) *Current Biol.* **7**, 844-849.

## Biographies

**Hedva Spitzer** received B.A degree from the Hebrew University in Jerusalem, and MA and Ph.D in Electrophysiology from the Hebrew University. She directs the Vision Research Lab in Biomedical Engineering department in Engineering faculty at Tel Aviv University. Her research interest in the recent years are concentrated on color, wide dynamic range and adaptation mechanisms with applications also to technology.

**Yuval Barkan** received his B.Sc. From Tel Aviv University in physics cummumum landa and B.Sc. in Electrical and electronical Engineering degree in 2002.